BldC delays entry into development to produce a sustained period of vegetative growth in *Streptomyces venezuelae*

Matthew J. Bush[1,*], Mahmoud Al-Bassam[1,#], Govind Chandra[1], Kim C. Findlay[2] and Mark J. Buttner[1]

[1]*Department of Molecular Microbiology*, and [2]*Department of Cell and Developmental Biology, John Innes Centre, Norwich Research Park, Norwich NR4 7UH, UK*.

* To whom correspondence should be addressed. Tel: 44 (0) 1603 450757; Fax: 44 (0) 1603 450778; Email:matt.bush@jic.ac.uk

[#] Current address: Department of Paediatrics, University of California, San Diego, La Jolla, CA 92093, USA

Keywords: Morphological differentiation; sporulation; cell division; transcriptional regulation.

Abstract

Streptomycetes are filamentous bacteria that differentiate by producing spore-bearing reproductive structures called aerial hyphae. The transition from vegetative to reproductive growth is controlled by the *bld* (bald) loci, and mutations in *bld* genes prevent the formation of aerial hyphae, either by blocking entry into development (mutations in activators) or by inducing precocious sporulation in the vegetative mycelium (mutations in repressors). One of the *bld* genes, *bldC*, encodes a 68-residue protein with a winged Helix-Turn-Helix (wHTH) DNA-binding motif. Here we exploit the benefits of the new model species, *Streptomyces venezuelae*, which sporulates in liquid culture, to study the biological role of BldC. Using electron microscopy and time-lapse imaging, we show that *bldC* mutants are bald because they initiate development prematurely, bypassing the formation of aerial hyphae. This correlates with premature expression of BldC target genes, showing that BldC acts as a repressor to sustain vegetative growth and delay entry into development.

Introduction

The complex *Streptomyces* life cycle involves two distinct filamentous cell forms: the growing or vegetative hyphae and the reproductive or aerial hyphae, which differentiate into long chains of spores (1-5). Genetic studies identified the regulatory loci that control entry into development, which are called *bld* (bald) genes because null mutations in these loci prevent the formation of aerial hyphae. However, baldness can arise for two different reasons. The larger class of *bld* mutants, which define positive regulators, fail to initiate development, forming colonies of undifferentiated vegetative mycelium. In contrast, a smaller but growing class of *bld* mutants, which define negative regulators, enter development prematurely, inducing sporulation in the vegetative mycelium and bypassing the formation of aerial hyphae. Thus, macroscopically these two classes of mutants look similar, forming smooth colonies that lack the 'hairy' appearance of the wild type, but microscopically it is apparent that they arise for diametrically opposed reasons (4, 6-8).

bldC is known to encode a short, 68 residue protein related to the DNA-binding domain of MerR-family proteins (9), but there has been less insight into its biological role and impact on *Streptomyces* development. In part, this is because previous studies have focussed on the classical model species, *S. coelicolor*, which sporulates only on solid medium. Here we exploit the benefits of the new model species, *Streptomyces venezuelae*, which sporulates in liquid culture (10), to study the biological role of BldC. We show that *bldC* mutants are bald because they enter development prematurely, bypassing the formation of aerial hyphae. This correlates with premature expression of BldC target genes, showing that BldC acts as a repressor to sustain vegetative growth and delay entry into development.

Results

Deletion of *bldC* causes premature initiation of development

We constructed an *S. venezuelae bldC* mutant by replacing the *bldC* coding region with an apramycin resistance (*apr*) cassette. The resulting mutant was bald, unable to produce the reproductive aerial hyphae that give mature wild-type *Streptomyces* colonies their characteristic fuzzy appearance (Fig 1.). However, scanning electron microscopy (SEM) of mature colonies of the *bldC* mutant showed that most of the biomass consisted of spores, rather than undifferentiated vegetative hyphae (Fig. 2). Comparison of the growth of the wild type and the *bldC* mutant on plates over time showed that after 1 day they looked similar (vegetative growth only) but after 2 days the wild type had produced aerial hyphae while the *bldC* mutant was still restricted to vegetative growth. After 3 days, the aerial hyphae of the wild-type had differentiated into spores, and most of the biomass of the *bldC* mutant had also differentiated into spores, bypassing aerial mycelium formation. The *bldC* mutant also seemed to produce higher levels of extracellular matrix than the wild type (Fig. 2). The *bldC* mutant phenotype was fully complemented by introducing a single copy of the *bldC* gene under the control of its native promoter, expressed *in trans* from the ΦBT1 integration site (Figs. 1 and 2).

Using an established microfluidic system and methodology (10), we conducted fluorescence time-lapse microscopy to further study the developmental defects associated with deletion of *bldC*. As in previous studies (6,10), we introduced an FtsZ-YPet translational fusion into the wild type, mutant and complemented mutant strains, enabling us to monitor each of the two distinct modes of cell division that occur in *Streptomyces*. In Fig. 3, the scattered single Z-rings mark the position of vegetative cross-walls, which do not constrict or give rise to cell-cell separation, but simply divide the vegetative hyphae into long, box-like compartments

64 (e.g. Figs. 3A + C, panel 2). In contrast, during reproductive growth, long ladders of regularly
65 spaced Z-rings are synchronously deposited along sporogenic hyphae. These Z-rings mark
66 the sites of sporulation septa, which do constrict, ultimately leading to the formation of chains
67 of spores (e.g. Figs. 3A + C, panels 3 +4). Time-lapse imaging of strains harbouring the FtsZ-
68 YPet fusion showed that the duration of vegetative growth was shorter in the *bldC* mutant
69 compared to the wild type and the complemented mutant (Fig.3 and Movies S1 A/B, S2 A/B
70 and S3 A/B). Noticeably, following germination, hyphal outgrowth in the *bldC* mutant was
71 associated with an immediate increase in FtsZ-YPet expression, leading to the precocious
72 formation of ladders of Z-rings (Fig. 3B and Movie S2A/B). However, although ladders of Z-
73 rings were observed as early as 4 hours in the *bldC* mutant, mature spores were not observed
74 in the corresponding DIC images until 21 hours, the same time mature spores were also seen
75 in the wild type (Figs. 3A and B). Wild-type patterns of FtsZ expression and sporulation were
76 restored in the complemented mutant (Fig. 3C and Movie S3A/B). From these data, we
77 concluded that the overall role of BldC is to sustain vegetative growth and delay entry into
78 development.
79
80 **BldC levels are highest early in development**
81 Using an anti-BldC polyclonal antibody, we monitored BldC levels in *S. venezuelae* during
82 sporulation in liquid culture. Western blotting showed that BldC is abundant throughout the
83 life cycle, but that BldC levels are highest early on, during vegetative growth (Figure 4).
84
85 **BldC represses transcription of its target genes**
86 ChIP-chip studies in *S. coelicolor* showed that BldC binds upstream of ~280 genes (11).
87 These targets include many genes encoding key transcriptional regulators of the *Streptomyces*
88 developmental cascade (e.g. *bldM*, *whiB*, *whiD*, *whiH*, *whiI*, *sigF* and *bldC* itself), as well as

89 others encoding proteins involved in chromosome condensation and segregation during
90 sporulation (e.g. *hupS*, *smeA-sffA*). Schumacher et al. (11) characterised the interaction of *S.*
91 *coelicolor* BldC with the promoters of two of its targets, *whiI* and the *smeA-ssfA* operon. *whiI*
92 encodes an orphan response-regulator that is essential for the later stages of sporulation, when
93 it forms a functional heterodimer with a second orphan response-regulator, BldM, enabling
94 WhiI to bind to DNA and regulate the expression of ~40 late sporulation genes (12). The
95 *smeA-sffA* operon encodes a small membrane protein (SmeA) that recruits a DNA translocase
96 (SffA) to sporulation septa (13). Deletion of *smeA-sffA* results in a defect in spore
97 chromosome segregation and has pleiotropic effects on spore maturation (13).

98 BldC binds directly to the *whiI* and *smeA* promoters in *S. coelicolor* (11) and ChIP-chip
99 analysis confirmed that they are also BldC targets in *S. venezuelae* (Table S1, Fig. 5). To
100 assess the regulatory influence of BldC on the *whiI* and *smeA* promoters, we performed qRT-
101 PCR using RNA prepared from both wild-type *S. venezuelae* and the *bldC* mutant, examining
102 the 8 and 10 hour time points when BldC is most abundant in wild-type cells (Fig. 5). In the
103 wild type, expression of both BldC targets comes on in the 10-h time point. In contrast, in the
104 *bldC* mutant, expression of both *whiI* and *smeA* is on in the 8- and 10-h time points.
105 Furthermore, at 10-h, expression of *whiI* is 15-fold higher in the *bldC* mutant compared to the
106 wild type and expression of *smeA* is 40-fold higher. Similarly, we conducted qRT-PCR to
107 assess the regulatory impact of BldC on the expression of three further key BldC targets - the
108 *sigF*, *whiD* and *hupS* genes. As we observed for *whiI* and *smeA*, expression of the *sigF*, *whiD*
109 and *hupS* genes comes on early in the *bldC* mutant (Fig. 6). We conclude that BldC functions
110 to repress the transcription of these developmental target genes during vegetative growth,
111 consistent with the premature initiation of development seen in a *bldC* mutant.
112
113

114 **Discussion**

115 Canonical *bld* mutations block entry into development and so the resulting colonies do not
116 form aerial hyphae and spores. Such mutations typically define positive regulators such as the
117 response regulator BldM (12) or the sigma factor BldN (14). In contrast, we have shown that
118 *S. venezuelae bldC* mutants are bald because they enter development prematurely, bypassing
119 the formation of aerial hyphae, and that this correlates with premature expression of BldC
120 target genes like *whiI* and *smeA*. Thus, BldC functions as a repressor to sustain vegetative
121 growth and delay entry into development. As such, BldC joins a growing class of Bld
122 regulators known to function as a developmental "brake".

123 BldD was the first Bld regulator of this alternative class to be clearly recognized. BldD sits at
124 the top of the developmental cascade and represses a large regulon of ~170 sporulation genes
125 during vegetative growth. BldD activity is controlled by the second messenger c-di-GMP,
126 which mediates dimerization of two BldD protomers to generate a functional repressor. In
127 this way, c-di-GMP signals through BldD to repress expression of the BldD regulon,
128 extending vegetative growth and inhibiting entry into development (4, 8, 15). Because it is a
129 BldD-(c-di-GMP) complex that represses the BldD regulon and not BldD alone, engineering
130 the degradation of c-di-GMP *in vivo* also causes a precocious hypersporulation phenotype
131 like that of a *bldD* null mutant (8).

132 More recently, *bldO* was identified as a second member of this emerging class of *bld* mutant
133 (6-7). In contrast to BldD and BldC, which both control large regulons, BldO functions to
134 repress a single developmental gene, *whiB*. The precocious hypersporulation phenotype of
135 the *bldO* mutant arises from premature expression of *whiB*, and in line with this, constitutive
136 expression of *whiB* alone is sufficient to induce precocious hypersporulation in wild-type *S.*
137 *venezuelae* (6). WhiA and WhiB act together to co-control the same set of promoters to
138 initiate developmental cell division in *Streptomyces* (16-17). WhiA is constitutively present

139 throughout the life cycle, but it only binds to its target promoters at the onset of sporulation
140 (16). This is because WhiA and WhiB function cooperatively and *in vivo* DNA binding by
141 WhiA depends on WhiB, and *vice versa* (17). As a consequence, the regulation of *whiB*
142 expression is key in controlling the switch between hyphal growth and sporulation. This
143 critical role for WhiB is reflected in the extensive developmental regulation to which *whiB*
144 transcription is subject, being directly repressed by BldC (11), BldD (18) and BldO (6), and
145 directly activated by BldM (12).
146

147 **Materials and Methods**

148 **Construction and complementation of an *S. venezuelae bldC* null mutant.** Using
149 'Redirect' PCR targeting (19-20), *bldC* mutants were generated in which the coding region
150 was replaced with a single apramycin resistance (*apr*) cassette. A cosmid library that covers >
151 98% of the *S. venezuelae* genome (M.J. Bibb and M.J. Buttner, unpublished) is fully
152 documented at http://strepdb.streptomyces.org.uk/. Cosmid 4O24 was introduced into *E. coli*
153 BW25113 containing pIJ790 and the *bldC* gene (*sven3846*) was replaced with the *apr-oriT*
154 cassette amplified from pIJ773 using the primer pairs bldCdis_F and bldCdis_R. The
155 resulting disrupted cosmids were confirmed by restriction digestion and by PCR analysis
156 using the flanking primers bldCcon_F and bldCcon_R, and introduced into *S. venezuelae* by
157 conjugation (Keiser *et al*., 2000). Null mutant derivatives, generated by double crossing over,
158 were identified by their apramycin-resistant, kanamycin-sensitive and morphological
159 phenotypes, and their chromosomal structures were confirmed by PCR analysis using the
160 flanking primers bldCcon_F and bldCcon_R. A representative *bldC* null mutant was
161 designated SV25. For complementation, *bldC* was amplified with the primers bldCcomp_F
162 and bldCcomp_R, generating an 846bp fragment carrying the coding sequence and the *bldC*
163 promoter, and cloned into HindIII-KpnI/Asp718 cut pIJ10770 to create pIJ10618. The

164 plasmid was introduced into the *bldC* mutant by conjugation and fully complemented all
165 aspects of the mutant phenotype.
166
167 **Time-lapse imaging of *S. venezuelae*.** Fluorescent time-lapse imaging was conducted
168 essentially as described previously (6,11). Before imaging, fresh *S. venezuelae* spores for
169 each of the strains imaged were first prepared by inoculating 30 ml cultures of MYM with 10
170 µl of the appropriate spore stock or 20 µl of the appropriate mycelial culture. Cells were
171 cultured at 30 ºC and 250 rpm until fully differentiated (16-24 h for hypersporulating strains,
172 otherwise 36-40 h). 1 ml of each culture was spun briefly to pellet mycelium, the supernatant
173 spores were diluted 1:50 in fresh MYM, and 50 µl was transferred to the cell loading well of
174 a prepared B04A microfluidic plate (Merck-Millipore). The remaining culture was filter-
175 sterilised to obtain spent MYM that was free of spores and mycelial fragments. The ONIX
176 manifold was then sealed to the B04A plate before transferring to the environmental
177 chamber, pre-incubated at 30 ºC. Spores were loaded onto the B04A plate, at 4 psi for 15
178 seconds using the ONIX microfluidic perfusion system. Fresh MYM medium was set to flow
179 at 2 psi during the first 3 hours during germination, before the 2-psi flow of spent MYM
180 medium for the remainder of the experiment. The system was left to equilibrate for 1 h prior
181 to imaging.
182
183 Imaging was conducted using a Zeiss Axio Observer.Z1 widefield microscope equipped with
184 a sCMOS camera (Hamamatsu Orca FLASH 4), a metal-halide lamp (HXP 120V), a
185 hardware autofocus (Definitive Focus), a 96-well stage insert, an environmental chamber, a
186 100x 1.46 NA Oil DIC objective and the Zeiss 46 HE shift free (excitation500/25 nm,
187 emission 535/30 nm) filter set. DIC images were captured with a 150 ms exposure time, YFP
188 images were captured with a 100 ms exposure time. Images were taken every 30 min. In all

189 experiments, multiple x/y positions were imaged for each strain and in each experiment.
190 Representative images were transferred to the Fiji software package (http://fiji.sc/Fiji),
191 manipulated and converted into the movie files presented here, as described previously
192 (Schlimpert *et al*., 2016).
193
194 **Chromatin immunoprecipitation-microarray (ChIP-chip) analysis.** To carry out the
195 ChIP-chip experiments, cultures of *S. venezuelae* and the congenic *bldC* null mutant strain
196 SV25 were grown for 12 h in MYM liquid medium. Formaldehyde was added to cultures at a
197 final concentration of 1% (v/v) and incubation was continued for 30 min. Glycine was then
198 added to a final concentration of 125 mM to stop the cross-linking. Cultures were left at room
199 temperature (RT) for 5 min before the mycelium was harvested and washed twice in PBS
200 buffer pH 7.4. Each mycelial pellet was resuspended in 0.5 ml lysis buffer (10 mM Tris HCl
201 pH 8.0, 50 mM NaCl) containing 15 mg/ml lysozyme and protease inhibitor (Roche Applied
202 Science) and incubated at 25 ºC for 1 h. An equal volume of IP buffer (100 mM Tris HCl pH
203 8, 250 mM NaCl, 0.5% Triton-X-100, 0.1% SDS) containing protease inhibitor was added
204 and samples were chilled on ice. Samples were sonicated for 7 cycles of 15 s each at 10
205 microns to shear the chromosomal DNA into fragments ranging from 300-1000 bp in size.
206 Samples were centrifuged twice at 13,000 rpm at 4 ºC for 15 min to clear the cell extract,
207 after which 10 µl of cell extract was set aside for total DNA extraction. The remainder was
208 incubated with 10% (v/v) protein A-sepharose (Sigma) for 1 h on a rotating wheel to remove
209 non-specifically binding proteins. Samples were then centrifuged for 15 min at 4ºC and
210 13,000 rpm to remove the beads. Supernatants were incubated with 10% (v/v) anti-BldC
211 antibody (9) overnight at 4 ºC with rotation. Subsequently, 10% (v/v) protein A-sepharose
212 was added to precipitate BldC and incubation was continued for 4 h. Samples were
213 centrifuged at 3500 rpm for 5 min and the pellets were washed four times with 0.5x IP buffer.

214 Each pellet was incubated overnight at 65 ºC in 150 µl IP elution buffer (50 mM Tris HCl pH
215 7.6, 10 mM EDTA, 1% SDS) to reverse cross-links, and 10 µl of the total cell extract control
216 was treated in the same way. Samples were centrifuged at 13,000 rpm for 5 min to remove
217 the beads. Each pellet was re-extracted with 50 µl TE buffer (10 mM Tris HCl pH 7.4, 1 mM
218 EDTA) and the supernatant incubated with 0.2 mg/ml Proteinase K (Roche) for 2 h at 55ºC.
219 The resulting samples were extracted with phenol-chloroform and further purified using
220 QiaQuick columns, eluting in 50 µl EB buffer (Qiagen). DNA labelling, hybridization to
221 DNA microarrays and data processing were carried out as described previously (10). All data
222 is deposited at ArrayExpress (Accession: E-MTAB-6129).
223
224 **qRT-PCR.** Mycelial pellets from MYM cultures were washed in PBS and resuspended in
225 900 µl lysis solution (400 µl phenol [pH4.3], 100 µl chlorophorm:isoamyl alcohol (24 : 1)
226 and 400 µl RLT buffer [Qiagen]) with lysing matrix B (MP Biomedicals) and homogenised
227 using a FastPrep FP120 Cell Disruptor (Thermo Savant). Two pulses of 30 s of intensity 6.0
228 were applied with cooling down for 1 min on ice between pulses. Supernatants were
229 centrifuged for 15 min, full-speed on a bench-top centrifuge at 4°C and then treated according
230 to the instructions given in the RNEasy Kit (Qiagen). The RNA samples were treated with
231 on-column DNase I (Qiagen), followed by an additional DNase I treatment (Turbo DNA-free,
232 Ambion) until they were free of DNA contamination (determined by PCR amplification of
233 *hrdB*). RNA was quantified and equal amounts (350 ng) of total RNA from each sample was
234 converted to cDNA using SuperScript II reverse transcriptase and random primers
235 (Invitrogen). cDNA was then used as template in qRT-PCR performed using the SensiFAST
236 SYBR No-ROX kit (Bioline). Three technical replicates were used for each gene. Specific
237 qPCR primers (Table S1, final concentration of 250 nM) were used to amplify the target
238 genes *whiI, smeA, whiD, sigF* and *hups,* as well as the *hrdB* reference gene. To normalize for

239 differing primer efficiency, a standard curve was constructed using chromosomal DNA.
240 Melting curve analysis was used to confirm the production of a specific single product from
241 each primer pair. qRT-PCR was performed using a CFX96 Touch instrument using hardshell
242 white PCR plates (BioRad), sealed with thermostable film covers (Thermo). PCR products
243 were detected with SYBR green fluorescent dye and amplified according to the following
244 protocol: 95°C, 3 min, then 45 cycles at 95°C 5 sec, 62°C 10 sec and 72°C 7 sec. Melting
245 curves were generated at 65 to 95°C with 0.5°C increments. The BioRad CFX manager
246 software was used to calculate starting quantity (SQ) values for *smeA* and *whiI* at each time
247 point. These values were divided by the mean SQ value derived from the *hrdB* reference at
248 the corresponding time points, generating a value for relative expression. The resulting values
249 were normalised against the mean relative expression of the wild type at 8 hours, which was
250 set to 1.
251
252 **Western Blotting.** Samples of frozen mycelium, originating from 2 ml liquid MYM samples,
253 were resuspended in 0.4 ml ice-cold sonication buffer [20 mM Tris pH 8.0, 5 mM EDTA, 1 x
254 EDTA-free protease inhibitors (Roche)] and sonicated (5x 15 sec on/15 sec off) at 4.5 micron
255 amplitude. Lysates were then centrifuged at 16,000 xg for 15 min at 4˚C to remove cell
256 debris. Total protein concentration was determined using the Bradford assay (Biorad). 1 µg of
257 total protein from each time point was loaded in triplicate into a microplate (proteinsimple
258 #043-165) and anti-bldC antibody (9) diluted 1:200. BldC levels, originating from the wild
259 type strain and the *bldC* mutant negative control were then assayed using the automated
260 Western blotting machine Wes (ProteinSimple, San Jose, CA), according to the
261 manufacturer's guidelines.
262

263 **Scanning electron microscopy.** Colonies were mounted on the surface of an aluminum stub
264 with optimal cutting temperature compound (Agar Scientific Ltd, Essex, UK), plunged into
265 liquid nitrogen slush at approximately -210°C to cryopreserve the material, and transferred to
266 the cryostage of an Alto 2500 cryotransfer system (Gatan, Oxford, England) attached to a FEI
267 NanoSEM 450 field emission gun scanning electron microscope (FEI Ltd, Eindhoven, The
268 Netherlands). The surface frost was sublimated at -95°C for 3½ mins before the sample was
269 sputter coated with platinum for 2 min at 10 mA at below -110°C. Finally, the sample was
270 moved onto the cryostage in the main chamber of the microscope, held at approximately -
271 130°C, and viewed at 3 kV.
272
273
274

Acknowledgements

We are grateful to Oxford Gene Technology for expert handling of the ChIP samples. This work was funded by BBSRC grant BB/H006125/1 (to M.J.B.) and by BBSRC Institute Strategic Programme Grant BB/J004561/1 to the John Innes Centre.

280 **References**

281 1. Flärdh K, Buttner MJ. 2009. *Streptomyces* morphogenetics: dissecting differentiation in a
282 filamentous bacterium. Nat Rev Microbiol 7: 36-49.

283 2. McCormick JR, Flärdh K. 2012. Signals and regulators that govern *Streptomyces*
284 development. FEMS Microbiol Rev 36: 206-231.

285 3. Jakimowicz D, and van Wezel GP. 2012. Cell division and DNA segregation in
286 *Streptomyces*: how to build a septum in the middle of nowhere? Mol Microbiol 85: 393-404.

287 4. Bush MJ, Tschowri N, Schlimpert S, Flärdh K, Buttner MJ. 2015. c-di-GMP signaling and
288 the regulation of developmental transitions in *Streptomyces*. Nat Rev Microbiol 13: 749-760.

289 5. Chater KF. 2016. Recent advances in understanding *Streptomyces*. F1000Res 5: 2795.

290 6. Bush MJ, Chandra G, Findlay KC, Buttner MJ. 2017. Multi-layered inhibition of
291 *Streptomyces* development: BldO is a dedicated repressor of whiB. Mol. Microbiol. 104: 700-
292 711.

293 7. Flärdh K, McCormick JR. 2017. The *Streptomyces* O-B one connection: a force within
294 layered repression of a key developmental decision. Mol. Microbiol 104: 695-699.

295 8. Tschowri N, Schumacher MA, Schlimpert S, Chinnam NB, Findlay KC, Brennan RG,
296 Buttner MJ. 2014. Tetrameric c-di-GMP mediates effective transcription factor dimerization
297 to control *Streptomyces* development. Cell 158: 1136-1147.

298 9. Hunt AC, Servin-Gonzalez L, Kelemen GH, Buttner MJ. 2005. The bldC developmental
299 locus of *Streptomyces coelicolor* encodes a member of a family of small DNA-binding
300 proteins related to the DNA-binding domains of the MerR family. J Bacteriol 187: 716-728.

301 10. Schlimpert S, Flärdh K, Buttner, MJ. 2016. Fluorescence time-lapse imaging of the
302 complete *Streptomyces* life cycle using a microfluidic device. J Vis Exp 108: e53863.

303 11. Schumacher MA, den Hengst CD, Bush MJ, Le TB, Tran NT, Chandra G, Zeng W,
304 Travis B, Brennan RG, Buttner MJ. 2017. Manuscript in preparation.

305 12. Al-Bassam MM, Bibb MJ, Bush MJ, Chandra G, Buttner MJ. 2014. Response regulator
306 heterodimer formation controls a key stage in *Streptomyces* development. PLoS Genet 10:
307 e1004554.

308 13. Ausmees N, Wahlstedt H, Bagchi S, Elliot MA, Buttner MJ, Flärdh K. 2007. SmeA, a
309 small membrane protein with multiple functions in *Streptomyces* sporulation including
310 targeting of a SpoIIIE/FtsK-like protein to cell division septa. Mol Microbiol 65:1458-1473.

311 14. Bibb MJ, Domonkos A, Chandra G, Buttner MJ. 2012. Expression of the chaplin and
312 rodlin hydrophobic sheath proteins in *Streptomyces venezuelae* is controlled by σ^{BldN} and a
313 cognate anti-sigma factor, RsbN. Mol. Microbiol. 84:1033–1049.

314 15. Schumacher MA, Zeng W, Findlay KC, Buttner MJ, Brennan RG, Tschowri N. 2017. The
315 *Streptomyces* master regulator BldD binds c-di-GMP sequentially to create a functional
316 $BldD_2$-$(c\text{-}di\text{-}GMP)_4$ complex. Nucleic Acids Res 45: 6923-6933.

317 16. Bush MJ, Bibb MJ, Chandra G, Findlay KC, Buttner MJ. 2013. Genes required for aerial
318 growth, cell division, and chromosome segregation are targets of WhiA before sporulation in
319 *Streptomyces venezuelae*. mBio 4: e00684-13.

320 17. Bush MJ, Chandra G, Bibb MJ, Findlay KC, Buttner MJ. 2016. Genome-wide chromatin
321 immunoprecipitation sequencing analysis shows that WhiB is a transcription factor that co-
322 controls its regulon with WhiA to initiate developmental cell division in *Streptomyces*. mBio
323 7: e00523-16.

324 18. den Hengst CD, Tran NT, Bibb MJ, Chandra C, Leskiw BK, Buttner MJ. 2010. Genes
325 essential for morphological development and antibiotic production in *Streptomyces coelicolor*
326 are targets of BldD during vegetative growth. Mol Microbiol 78: 361-379.

327 19. Gust B, Challis GL, Fowler K, Kieser T, Chater KF. 2003 PCR-targeted *Streptomyces*
328 gene replacement identifies a protein domain needed for biosynthesis of the sesquiterpene
329 soil odor geosmin. Proc Natl Acad Sci USA 100**:** 1541-1546.
330 20. Gust B, Chandra G, Jakimowicz D, Yuqing T, Bruton C, Chater KF. 2004. Lambda red-
331 mediated genetic manipulation of antibiotic-producing *Streptomyces*. Adv Appl Microbiol
332 54: 107-128.

333 **Figure Legends**

334 **FIG 1.** BldC is required for the formation of aerial mycelium.

335 The phenotypes of wild-type *S.venezuelae*, the *bldC* mutant, the *bldC* mutant carrying the
336 empty vector, and the complemented *bldC* mutant, photographed after four days of growth on
337 MYM solid medium.

338

339 **FIG 2.** Deletion of *bldC* causes premature initiation of development on solid medium.

340 Scanning electron micrographs showing the phenotype of the *bldC* mutant, compared to wild-
341 type after 1 days, 2 days and 3 days of growth on MYM solid medium. The phenotype of the
342 complemented *bldC* mutant is also shown after 3 days of growth on MYM solid medium.

343

344 **FIG 3.** Deletion of *bldC* causes premature initiation of development in liquid medium.

345 Time-lapse images (4, 7, 12 and 21 h post-inoculation) of (A) wild-type *S. venezuelae*, (B)
346 the *bldC* mutant and (C) the complemented *bldC* mutant, grown in liquid MYM medium in
347 the microfluidic system. All three strains carry the same FtsZ-YPet translational fusion
348 expressed from the native ftsZ promoter, and both the DIC (upper) and fluorescence (lower)
349 images are shown. Scale Bar = 10µm. For the corresponding movies, please see Supporting
350 Information Movies S1A/B, S2A/B and S3 A/B.

351

352 **FIG 4.** Automated Western blot analysis of BldC.

353 Equal amounts (1 µg) of total protein were loaded for each sample and BldC was detected
354 with polyclonal antibody (9) using the quantitative 'Wes' capillary electrophoresis and
355 blotting system (ProteinSimple – San Jose, CA). The *S. venezuelae bldC* mutant was used as
356 a negative control. Both the wild-type and *bldC* mutant were grown in MYM liquid medium.
357 (A) quantitation of BldO levels (area under each peak; arbitrary units). (B) virtual Western

358 blot. All experimental samples were analysed in triplicate and the mean value and its
359 Standard Error are shown for each sample. Each time-point is indicated in hours, along with
360 its relation to the developmental stage (V = vegetative growth; F = fragmentation; S =
361 sporulation), as determined by microscopy. Cultures used to analyse BldC levels were
362 identical to those used to prepare RNA prior to qRT-PCR analysis (Fig. 6).
363
364 **FIG 5.** BldC regulates the expression of many genes in *S. venezuelae*.
365 (A) Genome-wide distribution of BldC binding sites identified by ChIP-chip analysis using
366 anti-BldC polyclonal antibody, conducted during vegetative growth (12 hr) in the wild type.
367 DNA obtained from immunoprecipitation of BldC was labelled with Cy3 and hybridized to
368 DNA microarrays together with a total DNA control labelled with Cy5. Data are plotted as
369 Cy3/Cy5 ratios (y-axis), as a function of chromosome location (x-axis).
370 (B) ChIP-chip and qRT-PCR data for *whiI* and *smeA*. *Left Panels* - ChIP-chip in wild-type *S.*
371 *venezuelae* and the *S. venezuelae ΔbldC* mutant (blue and red dots, respectively). Plots span
372 approximately 8 kb of DNA sequence. *Right Panels* - mRNA abundance determined by qRT-
373 PCR in the wild type (white bars) and the *bldC* mutant (black bars). Strains were grown in
374 MYM liquid medium. Expression values were calculated relative to the accumulation of the
375 constitutively expressed *hrdB* reference mRNA and normalised to the wild-type value at 8 h.
376
377 **FIG 6.** ChIP-chip and qRT-PCR data for *sigF*, *whiD* and *hupS*. *Left Panels* - ChIP-chip in
378 wild-type *S. venezuelae* and the *S. venezuelae ΔbldC* mutant (blue and red dots, respectively).
379 Plots span approximately 8 kb of DNA sequence. *Right Panels* - mRNA abundance
380 determined by qRT-PCR in the wild type (white bars) and the *bldC* mutant (black bars).
381 Strains were grown in MYM liquid medium. Expression values were calculated relative to

382 the accumulation of the constitutively expressed *hrdB* reference mRNA and normalised to the

383 wild-type value at 8 h.

384

385

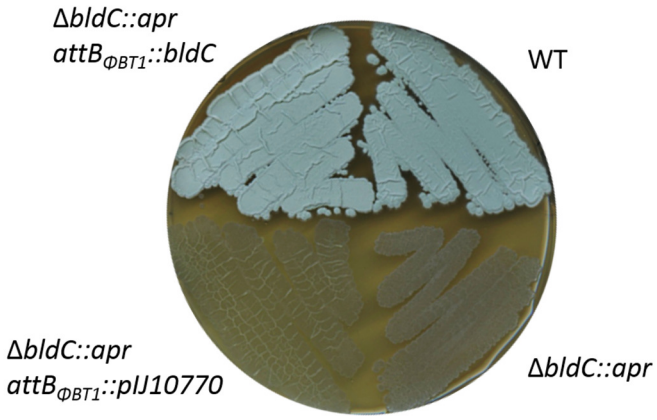
ΔbldC::apr
attB$_{\Phi BT1}$::bldC
WT
ΔbldC::apr
attB$_{\Phi BT1}$::pIJ10770
ΔbldC::apr

FIG 1

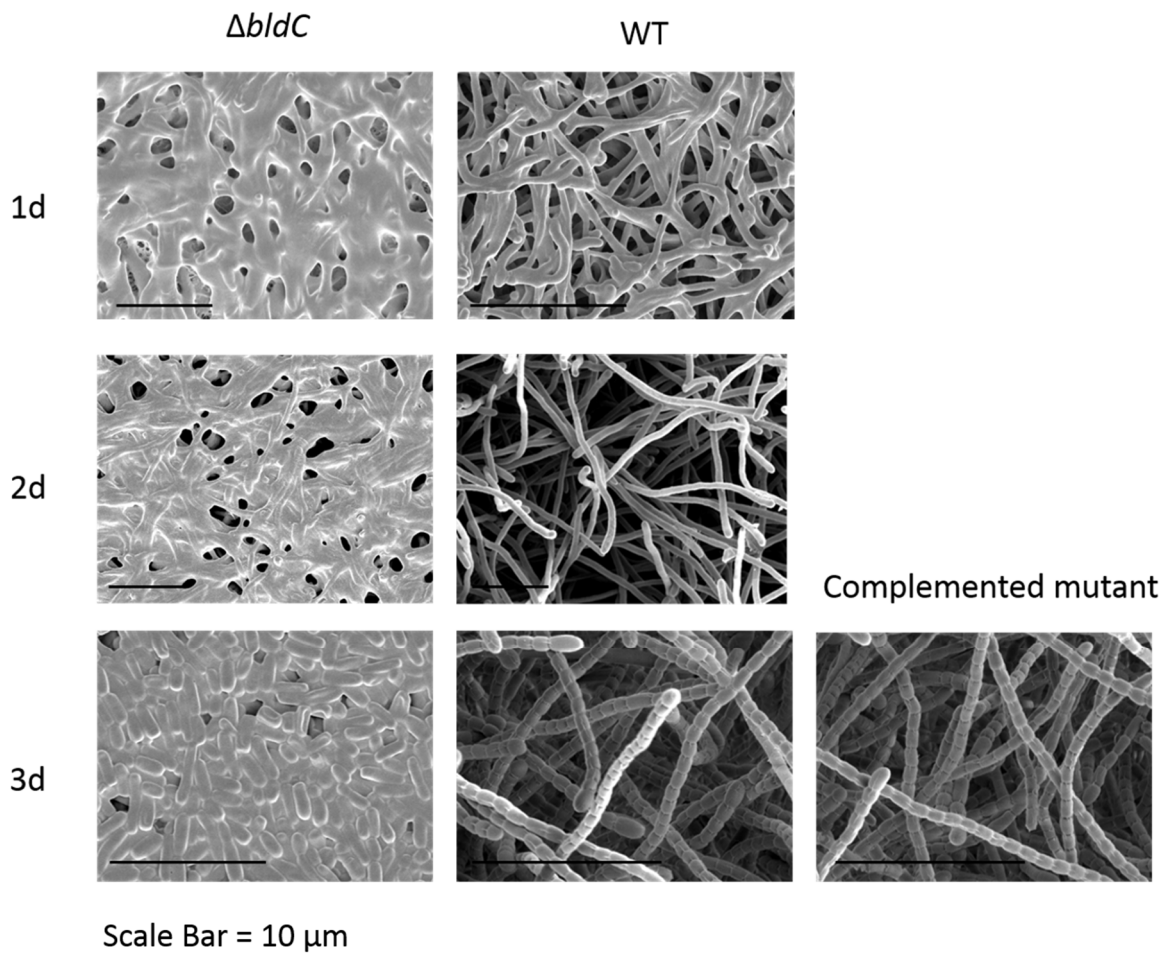

FIG 2.

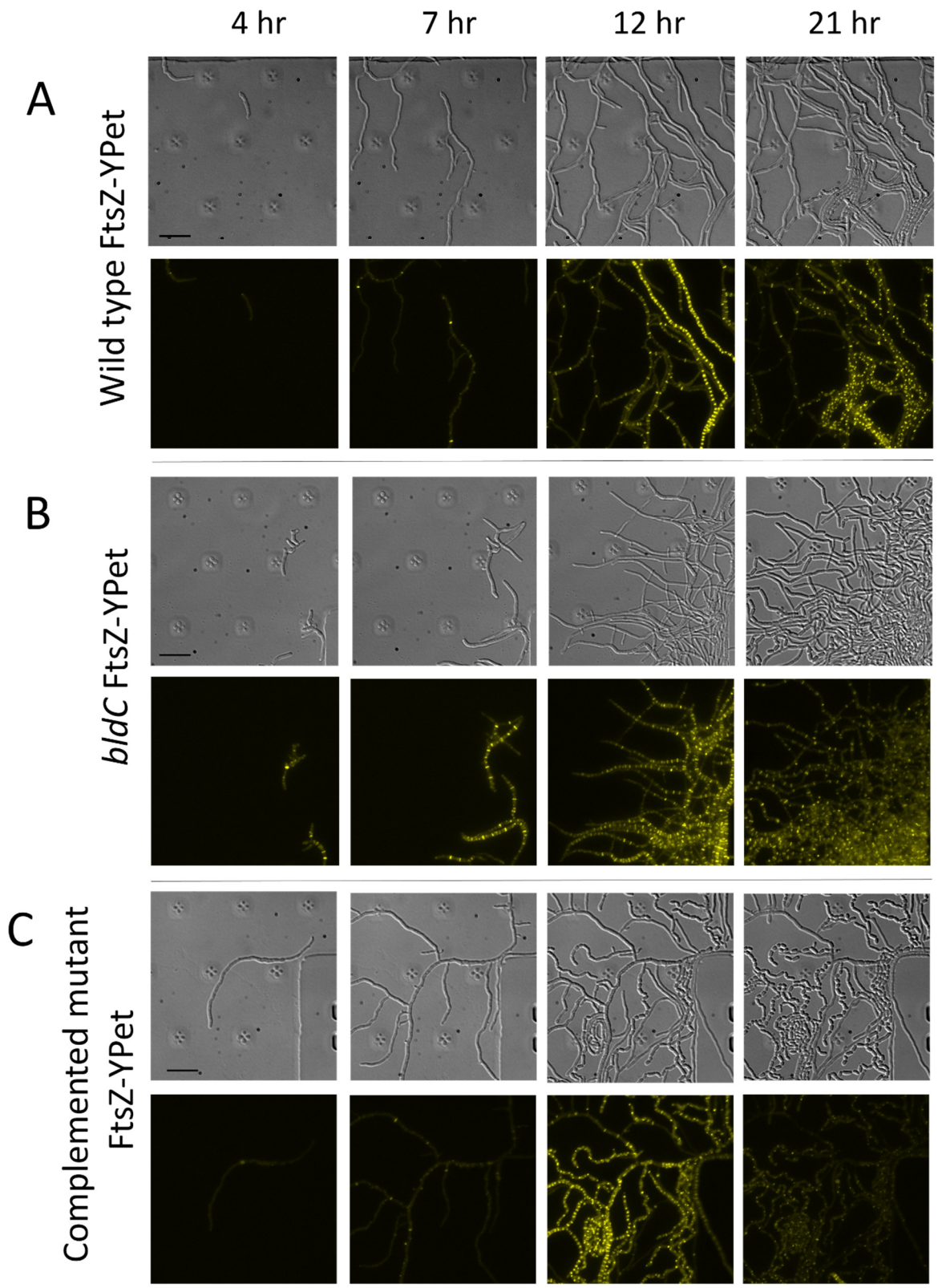
4 hr
7 hr
12 hr
21 hr
A
Wild type FtsZ-YPet
B
bldC FtsZ-YPet
C
Complemented mutant FtsZ-YPet

FIG 3.

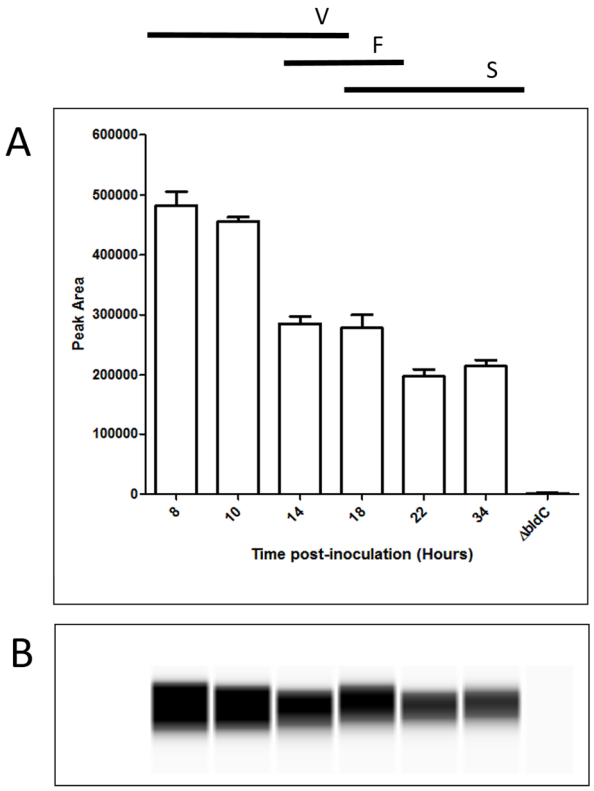
V
F
S
A
600000
500000
400000
300000
200000
100000
0
Peak Area
8
10
14
18
22
34
ΔbldC
Time post-inoculation (Hours)
B

FIG 4.

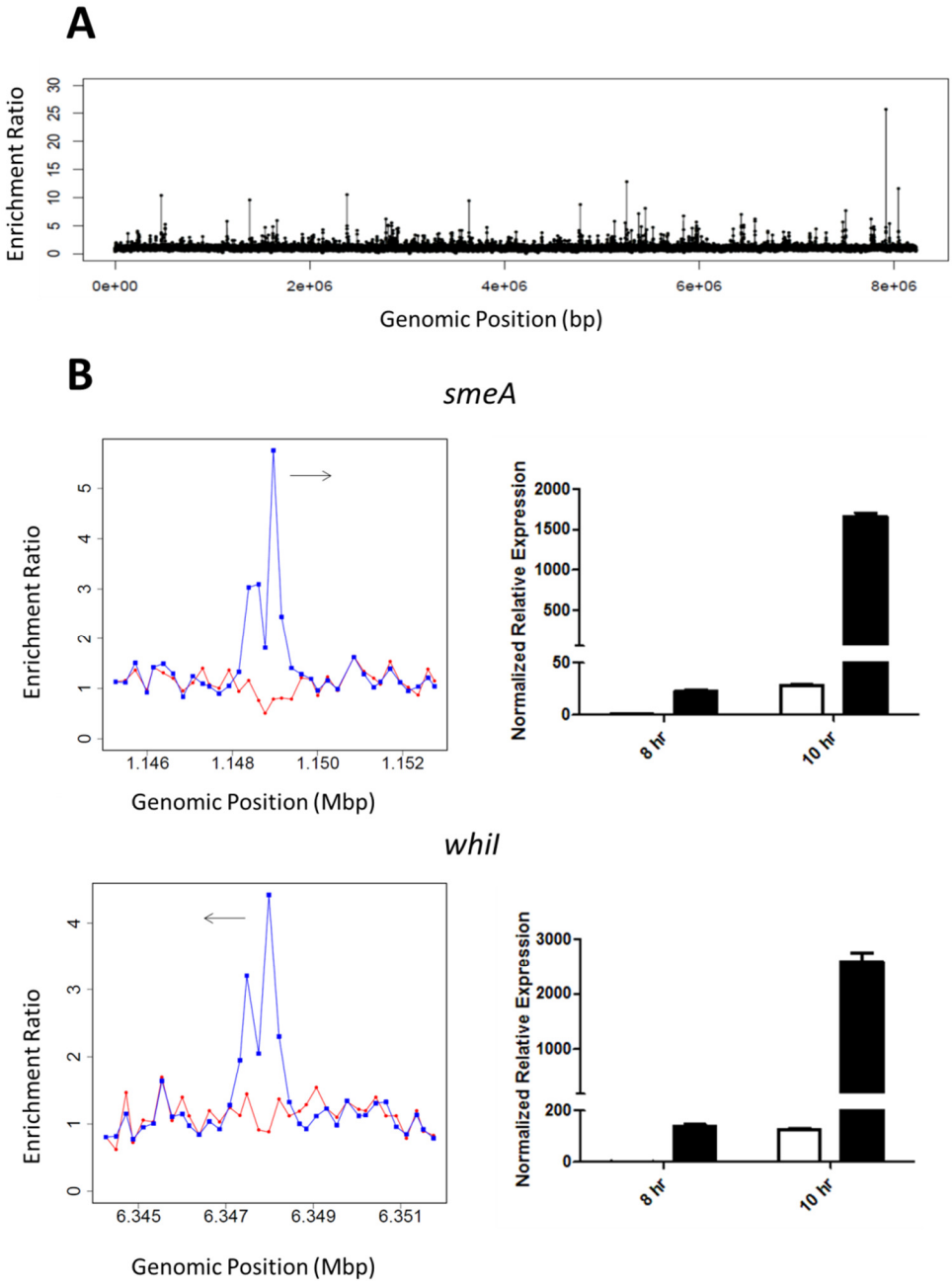
A
Enrichment Ratio
0
5
10
15
20
25
30
0e+00
2e+06
4e+06
6e+06
8e+06
Genomic Position (bp)
B
smeA
Enrichment Ratio
0
1
2
3
4
5
1.146
1.148
1.150
1.152
Genomic Position (Mbp)
Normalized Relative Expression
2000
1500
1000
500
50
0
8 hr
10 hr
whiI
Enrichment Ratio
0
1
2
3
4
6.345
6.347
6.349
6.351
Genomic Position (Mbp)
Normalized Relative Expression
3000
2000
1000
200
0
8 hr
10 hr

FIG 5.

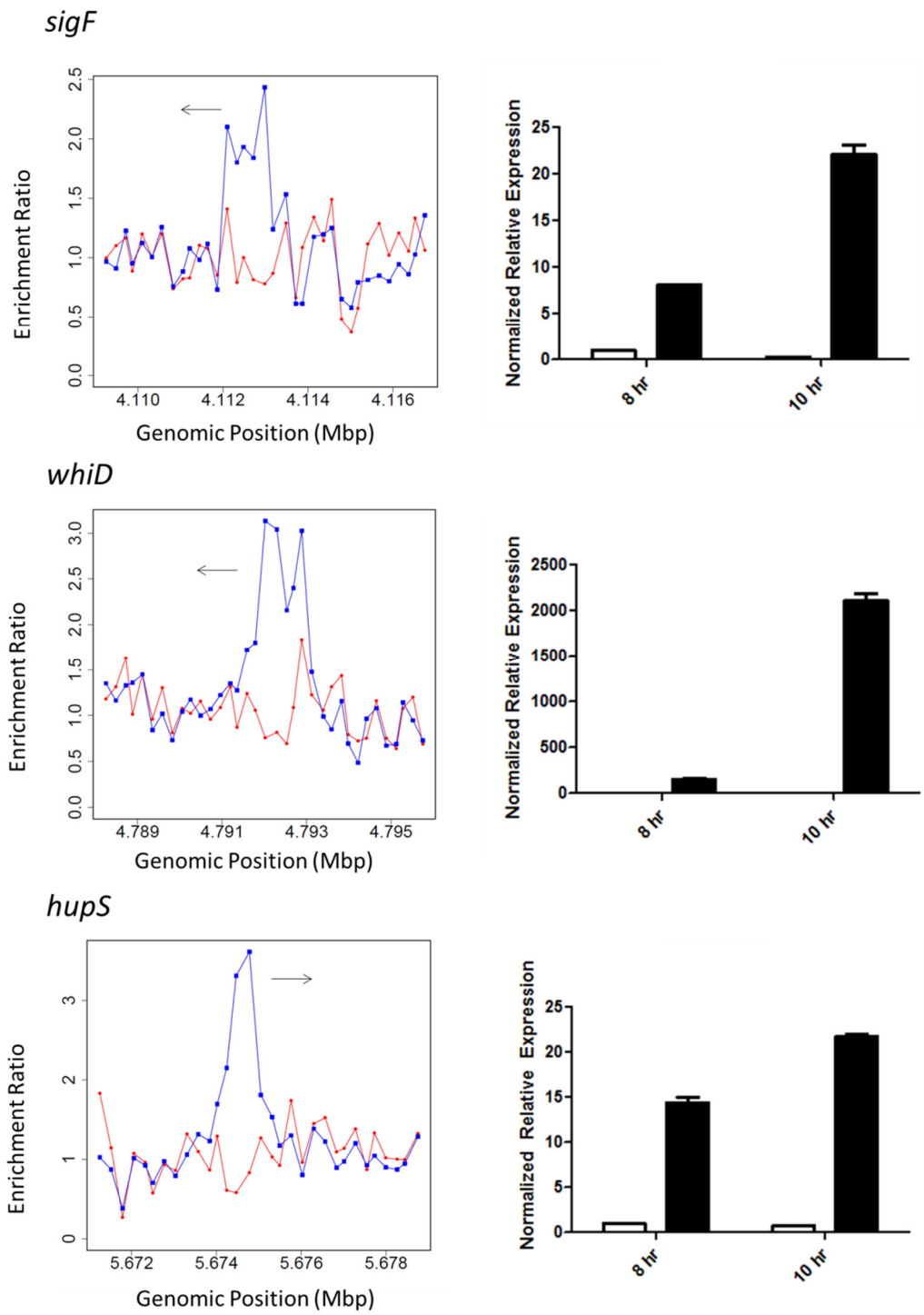
sigF
Enrichment Ratio
0.0
0.5
1.0
1.5
2.0
2.5
4.110
4.112
4.114
4.116
Genomic Position (Mbp)
Normalized Relative Expression
0
5
10
15
20
25
8 hr
10 hr
whiD
Enrichment Ratio
0.0
0.5
1.0
1.5
2.0
2.5
3.0
4.789
4.791
4.793
4.795
Genomic Position (Mbp)
Normalized Relative Expression
0
500
1000
1500
2000
2500
8 hr
10 hr
hupS
Enrichment Ratio
0
1
2
3
5.672
5.674
5.676
5.678
Genomic Position (Mbp)
Normalized Relative Expression
0
5
10
15
20
25
8 hr
10 hr

FIG 6.

386 **Supplemental Material**

387 **Table S1.** ChIP-chip data set for *S.venezuelae* BldC. Each row represents an enriched probe
388 (probeID) with the mid-position (midpos) of each probe on the *S. coilicolor* genome
389 recorded. Enrichment ratios are expressed as the log-fold change (logFC). Probes are listed in
390 order of significance (adjusted p value - adj.P.Val). For each probe, the nearest gene to the
391 left and right is identified (left/rightLocusTag), its distance to the midpos of the probe
392 (left/rightDistance), whether the gene is on the forward (1) or reverse (-1) strand (inStrand)
393 and the predicted function (left/rightProduct) based on annotation in strepdb
394 (http://strepdb.streptomyces.org.uk). If the midpos of a probe falls within a gene, it's gene
395 identifier (inLocusTag), distance to the probe (inDistance), whether the gene is on the
396 forward (1) or reverse (-1) strand (inStrand) and predicted function (inProduct) is also listed.

397

398 **Table S2.** Strains, Plasmids and Oligonucleotide primers used in this study

399

400 **Movie S1.** Time-lapse microscopy of the wild type strain carrying the FtsZ-YPet fusion. DIC
401 (A) and YFP-channel (B) movies are at 5 frames per second. The time following the first
402 image is indicated at the bottom left. Images were taken every 30 minutes (DIC 150 ms; YFP
403 100 ms). Movies were assembled in the Fiji software package (http://fiji.sc/Fiji).

404

405 **Movie S2.** Time-lapse microscopy of the *bldC* mutant carrying the FtsZ-YPet fusion. DIC
406 (A) and YFP-channel (B) movies are at 5 frames per second. The time following the first
407 image is indicated at the bottom left. Images were taken every 30 minutes (DIC 150 ms; YFP
408 100 ms). Movies were assembled in the Fiji software package (http://fiji.sc/Fiji).

409

410 **Movie S3.** Time-lapse microscopy of the complemented strain carrying the FtsZ-YPet fusion.
411 DIC (A) and YFP-channel (B) movies are at 5 frames per second. The time following the first
412 image is indicated at the bottom left. Images were taken every 30 minutes (DIC 150 ms; YFP
413 100 ms). Movies were assembled in the Fiji software package (http://fiji.sc/Fiji).
414